



Functionalization of polypropylene hollow fiber membrane with amino groups and its application for the removal of gold ions from wastewater solutions

Changkun Liu^{a,b,*}, Lin Wang^{a,b}, Xiaobin Lei^{a,b}, Jizhen Jia^{a,b}, Zhe Xu^a, Zhitao Ai^a, Xiaoyan Chai^{a,*}

^aCollege of Chemistry and Environmental Engineering, Shenzhen University, Shenzhen, China, emails: liuck@szu.edu.cn (C. Liu), chaixy@szu.edu.cn (X. Chai), 782792504@qq.com (L. Wang), 826798147@qq.com (X. Lei), 1195866282@qq.com (J. Jia), xuzhe.xz@foxmail.com (Z. Xu), 752112569@qq.com (Z. Ai)

^bShenzhen Key Laboratory of Environmental Chemistry and Ecological Remediation, Shenzhen 518060, China

Received 8 December 2017; Accepted 12 November 2018

ABSTRACT

This study investigated the aminated polymer brush-grafted polypropylene hollow fiber membrane via the grafting and the subsequent amination of the poly(glycidyl methacrylate) for the efficient and selective adsorption of trivalent gold ions (Au(III), in the form of AuCl_4^-). The prepared membrane was characterized by using Fourier Transform infrared spectroscopy, field-emission scanning electron microscopy, X-ray photoelectron spectroscopy, and water contact angle measurements. The membrane was successfully explored to study the adsorption performance of Au(III). Experimental results showed that the polymer brush grafting time of 4 h and the amination time of 12 h were the optimized synthesis conditions for the preparation of the aminated polypropylene hollow fiber membrane. The optimum pH for Au(III) adsorption onto the aminated polypropylene hollow fiber membrane was 2.5, with a fast adsorption kinetics which can be fitted by the pseudo-second-order kinetics model, and showed the maximum adsorption capacity of 2.7 mmol/g, as derived from the good fit of the Langmuir isotherm model. In addition, the aminated polypropylene hollow fiber membrane showed excellent adsorption selectivity toward trivalent gold ions over divalent zinc ions (in Au(III)/Zn(II) binary system). The prepared aminated polypropylene hollow fiber membrane would be suitable for the reclamation of the Au(III) ions as the precious heavy metal ions via the combination of adsorption and membrane technology.

Keywords: Polypropylene hollow fibre membrane; Diethylenetriamine; Selectivity; Adsorption; Au(III) ion; Polymer brush grafting; SI-ATRP; Poly(glycidyl methacrylate)

1. Introduction

Metal resources are the valuable wealth in the earth, which lay an indispensable foundation and play an important role in the economic development. With the advancement of the industrialization and the acceleration of the resource consumption, large quantities of different metal wastes would be expected to be fully recycled, reprocessed, and regenerated so that their original functions can be restored. If valuable metal ions from wastes can be recycled, over-exploitation of primary

metal resources can be mitigated, plenty of energies can be saved, and reutilization of resources can be fulfilled. Gold, as one of the precious metals with low reserves in the earth's crust, has unique characteristics with extensive application scope in several technical fields including electronics, communication, medical technology, etc.[1–3]. Gold often coexists with other heavy metals in a wide variety of sources, including wastewater from mining effluents, electronic waste disposal, gold plating, smelting industries, etc. However, many chemical compounds containing gold with high concentrations may be hazardous to organisms and environment [4]. Based on such

* Corresponding authors.

status quo, waste treatment and recycling of gold from heavy metal wastewater have more practical significance. Efficient treatment should be carried out on the recovery of gold from industrial wastewaters for the reuse of the valuable resource as well as the prevention of the environmental pollution.

Currently, the methods used for recycling of gold from industrial wastewaters include precipitation, solvent extraction, electrodeposition, and adsorption. The conventional chemical precipitation processes may be difficult to meet the increasingly stringent environmental regulations [5]. Solvent extraction method is usually used for the chemical analyses of the gold concentrations. Electrodeposition method is often used in gold leaching fluids with high concentrations, and it shows limitations for wastewaters with trace amounts of gold. In addition, the abovementioned methods may have some limitations such as the poor selectivity and difficulty in recyclability [6]. However, the wastewater containing gold from various industries may contain other heavy metal ions, and the selective separation of gold from it is of great significance. For example, the gold-containing electroplating wastewater often contains copper and zinc ions. The selective separation of gold would favor the reuse of the precious metal and thus become a key issue in resource recycling. Therefore, with the development of industry and the enhancement of the environmental protection awareness, much attention has been focused on the adsorption methods for wastewater treatment. The adsorption method shows great flexibility in operation and design with high heavy metal ion removal efficiency, and is easy for repeated use. [5,7–9]. Many materials (i.e., biomaterials, activated carbon, nanoparticles, rubber waste, carbon nanotubes, etc.) have been used as effective adsorbents, and a lot of research work has been carried out in developing novel adsorbents [10]. Polypropylene hollow fiber membrane (PPHFM) is a membrane material extensively applied in the field of water and wastewater treatment, featuring good impact resistance, wear resistance, corrosion resistance, large specific surface area, and decent separation efficiency. Traditional PPHFM, with only the physical property of intercepting particles, does not have the property of chemical adsorption, which limits its application for a broad range of pollutants. Therefore, if chemical adsorption property has been incorporated to PPHFM by means of surface chemical modification, its application would be greatly broadened not only for micro- or nano-sized particle removal but also for heavy metal ion adsorptive treatment. Amine functional groups are efficient functional groups for the adsorption of heavy metal ions, and would form the complexes with gold(III) for the removal of gold from aqueous solutions [11]. For example, Ramesh et al. [12] prepared glycine-modified crosslinked chitosan resin to adsorb gold(III) with the maximum adsorption capacity of 169.98 mg/g. Lin et al. [13] recovered Au(III) selectively from aqueous solutions using 2-aminothiazole functionalized corn bract as a low-cost bio-adsorbent. However, there was little research work on the amine-modified PPHFM for gold(III) adsorption. The amination of PPHFM would not only extend the applications of PPHFM into the adsorption field, but also enlighten the research fields of other multi-functional hollow fiber membrane materials.

Polymer brush grafting is one of the promising methods among chemical modifications [14,15], which can effectively change the chemical and physical properties of the material

surface. Through all kinds of active controllable polymerization, the variability of polymer brush structure can be realized, and thus, its usage in practice can be expanded. Therefore, new adsorbents for the precious metal ion sequestration can be tailor-made through the grafting of polymer brush capable of selective adsorption of the target precious metal ions. Such new adsorbents play an instructive role in controlling heavy metal ion pollution and recycling of precious metal resources. In many published literature, different strategies for grafting polymer brushes were described. Among them, the surface-initiated atom transfer radical polymerization (SI-ATRP) method has been extensively studied, which is able to achieve both high grafting density and high stability of polymer brush layer [16–18]. Compared with the conventional polymerization methods, SI-ATRP can provide controllable molecular weight and molecular weight distribution of the grafted polymer brush [19]. Therefore, SI-ATRP is one of the most efficient polymerization techniques for the grafting of various polymer brushes onto the substrates [20–23].

In this study, PPHFM was used as the substrate material for the grafting of the poly(glycidyl methacrylate) (PGMA) polymer brush via the SI-ATRP method, and subsequently the epoxy groups of the PGMA were reacted with diethylenetriamine (DETA). As to the best of our knowledge, the aminated polymer brush-modified PPHFM has not been reported for the selective adsorption of Au(III). This study elaborated the characteristic analyses of the aminated PPHFM and explore its selective adsorption property for Au(III) in gold and zinc binary species system. Moreover, this study would provide means of preparing selective adsorbents for gold ions using an industrially applied material PPHFM as the substrate and PGMA as the polymer brush which can be aminated in mild reaction conditions. Such adsorbents would be suitable for the reclamation of the precious Au(III) ions by the combined techniques of adsorption and membrane separation.

2. Experimental procedure

2.1. Materials

PPHFM was provided by Yuanxiang Technology Co., Ltd., Shenzhen, China. 2-bromide isobutyl bromide (BIBB, 98%), pyridine (AR), 2,2-bipyridine (BPy, 99%), cuprous bromide (CuBr, 99%), copper bromide (CuBr₂, 99%), glycidyl methacrylate (GMA, 97%), *N,N*-dimethylformamide (DMF, AR), DETA (99%), and tetrahydrofuran (THF, 99%) were all purchased from Shanghai Aladdin Reagent Co., Ltd., Shanghai, China. Chloroauric acid (HAuCl₄, AR) and ZnCl₂ (AR) was purchased from Sinopharm Chemical Reagent Co., Ltd., Shanghai, China. Stock solutions of 4 mmol/L containing Au and Zn ions were prepared. The pH at the range of 1–3 was adjusted using hydrochloric acid. Thiourea (AR, 99%), hydrogen peroxide solution (AR, 30%), and all other reagents were of analytical grade.

2.2. Grafting of PGMA polymer brush

Before grafting the PGMA by SI-ATRP technique, the bromination reaction on PPHFM was carried out to obtain the brominated PPHFM (denoted as PP-Br) [24–26]. The preparation steps were as follows: 0.1 g PPHFM was placed in a

plasma cleaner, and the surface was activated with plasma in air atmosphere for 5 min to generate the surface hydroxyl groups. Subsequently, 0.1 g of the activated PPHFM was placed into a test tube with 15 mL DCM. Then, 3 mL BIBB and 1 mL pyridine were added in the test tube which was placed in an ice-water bath. The tube was sealed, and the bromination reaction was carried out under magnetic stirring at a speed of 300 rpm for 24 h at room temperature. After the reaction, the fiber membrane was taken out, washed with acetone for 20 min and with deionized water for 10 min, and dried in a vacuum oven to obtain the PP-Br.

For SI-ATRP polymerization, 0.1 g of PP-Br was placed in a test tube and degassed with argon for 20 min. Afterward, 0.11 g CuBr, 0.03 g CuBr₂, and 0.2 g BPy were added in the test tube, followed by the addition of 2 mL deionized water, 4 mL DMF, and 6 mL GMA. The solution mixture was again degassed with argon for 10 min. After that, the test tube was sealed, and the SI-ATRP of PGMA polymer brush was carried out at the stirring speed of 150 rpm at the reaction temperature of 45°C for 4 h. After the reaction, the fiber membrane was taken out and washed with THF, 0.1 M HCl, 0.1 M NaOH, and deionized water and finally dried in vacuum oven to obtain the PPHFM with PGMA polymer brush grafted on the surface (denoted as PP-PGMA).

2.3. Amination

0.1 g PP-PGMA was added in a test tube, followed by the addition of 6 mL THF and 6 mL DETA. The test tube was sealed, and the amination reaction was carried out at a speed of 150 rpm for a specific period of time at room temperature. After the reaction was completed, the fibrous membrane was taken out and washed with acetone and deionized water and dried in vacuum oven to obtain the aminated PPHFM as the final product in this study (denoted as aminated PP). The schematic diagram of the surface functionalization of PPHFM is shown in Fig. 1.

2.4. Material characterization

The surface chemical functional groups of the original and modified PPHFM membranes were analyzed with Vertex 70 ATR-FTIR spectrometer (Bruker Corporation, Germany). The surface morphology of the membranes was observed with

field-emission scanning electron microscope (FESEM, JSM-7800F, JEOL, Japan). The surface element compositions of the membranes were identified, and the corresponding atom percentage was tested with the X-ray photoelectron spectrometer (XPS, ESCALAB 250Xi, Thermo, USA). The water contact angle (WCA) of the membrane surface was tested with the WCA testing instrument (SD-S1, Shengding, China).

2.5. Adsorption performance evaluation

The adsorption experiments were carried out in both single species (only Au(III) was present in the solution) and binary species (both Au(III) and Zn(II) were present in the solution) systems with the aminated PP. The concentrations of Au(III) and Zn(II) ions before and after the adsorption experiments were determined using inductive coupling plasma optical emission spectrograph (ICP-OES, Optima 2100DV, PerkinElmer, USA). The adsorption capacity was calculated according to Eq. (1):

$$q = \frac{(C_0 - C) \times V}{m} \quad (1)$$

where q (mmol/g) is the adsorption capacity, C_0 and C (mmol/g) are the initial and final concentrations of the heavy metal ion, respectively, V (L) is the volume of adsorption solution, and m (g) is the mass of the adsorbent.

To study the influence of the pH, 30 mg aminated PP samples were put into 30 mL Au(III) ion single or binary species solutions (with pH values being adjusted in the range of 1–3, and the initial concentration of 4 mmol/L for each of the heavy metal ions). When the pH was higher than 3.5, hydroxide precipitates would be formed in the solution [27–29]. The adsorption was carried out for 24 h at 25°C (the adsorption time significantly exceeded the time for the adsorption equilibrium).

To investigate the adsorption kinetics, 300 mg aminated PP was put into 300 mL Au(III) ion single or binary species solutions for the adsorption at the stirring speed of 150 rpm at 25°C. The samples were taken at different time intervals during heavy metal ion adsorption for ICP-OES analyses, with the adsorption capacity at different time intervals calculated according to Eq. (1).

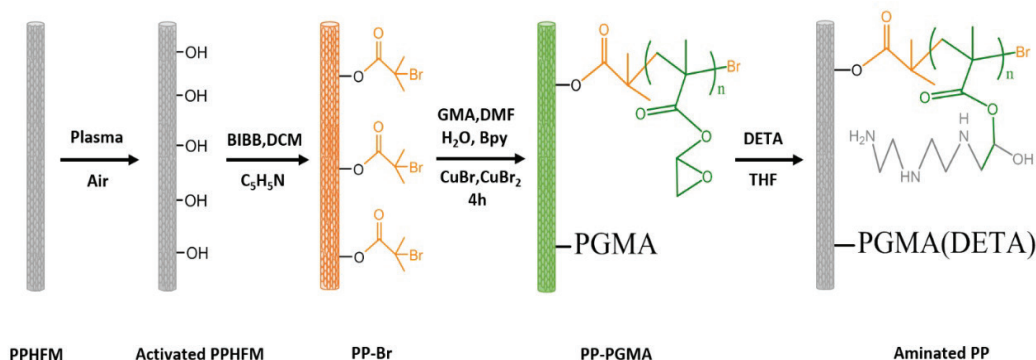


Fig. 1. Schematic diagram of the surface functionalization of PPHFM.

To investigate the adsorption isotherm, 30 mg aminated PP was put into 30 mL Au(III) ion single or binary species solutions with the initial concentration ranging from 0.2 to 4.0 mmol/L for each of the heavy metal ions, at the stirring speed of 150 rpm at 25°C. The initial and final Au(III) ion concentrations were measured using ICP-OES, and the equilibrium adsorption capacity was calculated.

2.6. Desorption and repeated-use experiments

For the desorption experiments, the thiourea solution was used as the desorption agent for the desorption of Au(III) from the Au(III)-adsorbed aminated PP. The Au(III) desorption was carried out in 20 mL of 0.1 mol/L thiourea solutions with the solid-to-liquid ratio (the ratio of the weight of the aminated PP to the volume of the thiourea solution) in the range of 0.3:1 to 6:1 (aminated PP with the weight of 6, 10, 20, 40, 60, 80, and 120 mg, respectively) and for a desorption time of 24 h at room temperature. The desorption efficiency was calculated using the following Eq. (2) [30]:

$$DE = \frac{C_{el}V}{q_{el}m} \times 100\% \quad (2)$$

where q_{el} (mmol/g) is the concentration of gold ions adsorbed on the adsorbents before the desorption experiment, C_{el} (mmol/L) is the gold ion final concentrations in thiourea solution after the desorption process, V (L) is the volume of the thiourea solution, and m (g) is the weight of the adsorbent.

For the repeated-use experiment, the Au(III) adsorption was first carried out with the solid-to-liquid ratio of 1:1, and in Au(III) solution with the initial concentration of 0.05 mmol/L. After the adsorption experiments, the Au(III)-adsorbed aminated PP was desorbed with the solid-to-liquid ratio of 1:1 for 24 h, and subsequently washed with 0.5 mol/L NaOH solution and deionized water, which was ready for use for the next cycle of adsorption–desorption. The cycle was repeated five times to examine the Au(III) removal efficiency and desorption efficiency.

3. Results and discussion

3.1. Functionalization of the PPHFM

The synthesis of the aminated PP is shown in Fig. 1. The hydroxyl groups on the activated PPHFM first reacted with BIBB to obtain the PP-Br, which can be regarded as the macro-initiator for the following PGMA polymerization by the SI-ATRP method. The obtained PP-PGMA was subsequently reacted with DETA by ring-opening reaction for the immobilization of DETA.

3.1.1. Grafting PGMA polymer brush

The optimum grafting time for PGMA polymer brush was investigated. A series of grafting time was selected for the grafting of the PGMA polymer brush, followed by the amination reaction for 48 h to ensure a complete reaction of the epoxy groups of PGMA with DETA. The prepared aminated membranes were examined with the element analyzer (VARIO EL cube, Germany) for the determination of the nitrogen content, which indirectly denoted the amount of the successfully grafted PGMA polymer brush [31].

Fig. 2(a) shows that the nitrogen content increased with the increase of the SI-ATRP time during the first 4 h and remained almost stable when the SI-ATRP time was further increased. As the nitrogen content can be regarded as the representative of the grafted polymer chain length [32,33], it can be concluded that the grafting time of 4 h was suitable for the SI-ATRP of the PGMA polymer brush. After the SI-ATRP technology, DETA was immobilized on the prepared PP-PGMA via the ring-opening reaction.

3.1.2. Amination process

The best amination time was also investigated. Different amination time was selected, and the prepared membranes were examined for the nitrogen contents with the element analyzer. The amination time corresponding to the highest nitrogen content was selected as the best amination time for the preparation of the aminated PP.

Fig. 2(b) shows the effect of the amination time on the nitrogen content of the aminated PP. The nitrogen content

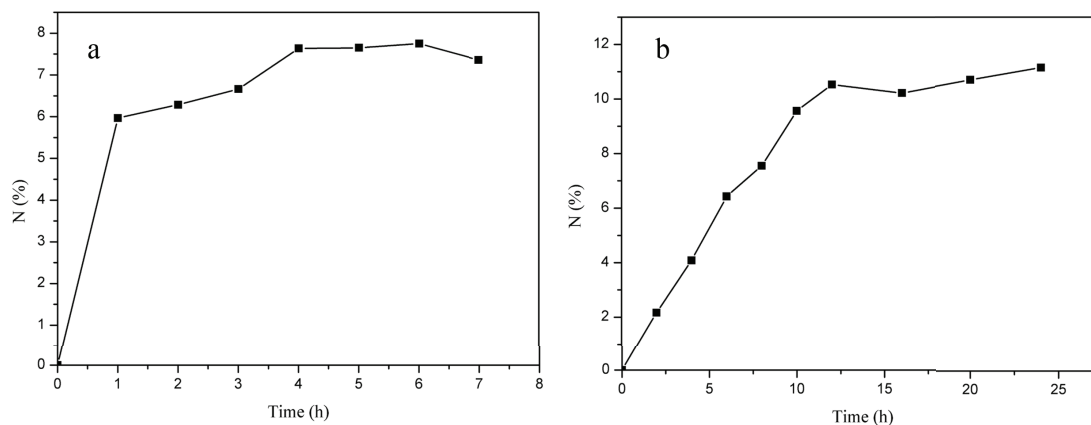


Fig. 2. (a) Nitrogen content (N%) of the aminated PP at different PGMA grafting time and (b) nitrogen content (N%) of the aminated PP at different amination times.

showed an increase with the increase of the amination time for the first 12 h and remained almost constant for the reaction time from 12 to 24 h. As a result, the suitable amination time was determined to be 12 h. Therefore, the PGMA grafting time of 4 h via SI-ATRP and the subsequent amination time of 12 h were determined to be the suitable synthesis conditions for the aminated PP.

3.2. Characterization of aminated PP

In order to prove the success of grafting and amination, ATR-FTIR was used for the surface functional group analyses of PPHFM before and after surface modification. As shown in Fig. 3, after grafting PGMA polymer brushes onto PPHFM forming PP-PGMA, a new peak at $1,728\text{ cm}^{-1}$ occurred which was attributed to the stretching vibration of the carbonyl (C=O) groups of the PGMA. In addition, the two peaks at 906 and 840 cm^{-1} were attributed to the stretching vibration of the epoxy groups of PGMA [34,35]. Therefore, the appearance of these characteristic peaks indicated the successful grafting of the PGMA polymer brush onto the PPHFM surface [36,37]. After the amination reaction, a broad peak appeared in the range of $3,000\text{--}3,700\text{ cm}^{-1}$ for the aminated PP, which was usually deemed as the combination of the stretching vibrations of the hydroxyl and amine groups [26]. And a new peak appeared at $1,565\text{ cm}^{-1}$ attributed to the deformation vibration of the amine groups [38]. These results indicated that the amine groups have been successfully introduced to the surface of PPHFM.

Hydrophilicity of the adsorptive membranes is usually required for the efficient adsorption of the heavy metal ions from waters and wastewaters. Therefore, the WCA was used to evaluate the hydrophilicity of the prepared membranes. As shown in Fig. 4, the WCA of the original PPHFM was 85° , showing lower hydrophilicity. After the plasma treatment, the WCA dropped to 0° due to the plenty of hydroxyl groups formed on the membrane surface [39]. The WCA of PP-Br was increased to 107° , due to the ester groups generated from the reaction between the hydroxyl groups of the

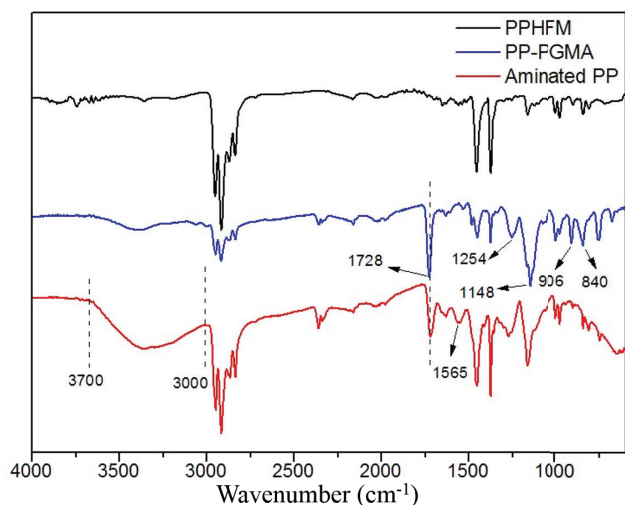


Fig. 3. ATR-FTIR spectra of PPHFM, PP-PGMA, and aminated PP.

plasma-treated PPHFM and the acyl bromide groups of BIBB [40]. After the amination reaction, the WCA dropped to 0° again due to the introduced DETA groups, indicating that the aminated PP would be favorable for the adsorption of heavy metal ions.

The FESEM images of PPHFM before and after the surface modification are shown in Fig. 5 to observe the effect of the surface modification on the surface morphology of the samples. The surface of the original PPHFM as microfiltration membrane was porous in high-magnification observation. In comparison, the aminated PP showed obvious roughness and wrinkles on the porous membrane surface, which indicated that the grafting of PGMA polymer brush and the subsequent amination was likely to change the surface morphology. This morphological change was also consistent with other reports [19]. The surface morphologies of the membranes before and after the surface modification indicated that the amination reaction was prone to change the surface morphologies of the PPHFM membranes.

3.3. Adsorption of Au(III)

3.3.1. Adsorption mechanisms

In acidic solution (HCl media), AuCl_4^- can be in combination with an amine either by coordination with the neutral amine of the aminated PP (Eq. (3)) or by electrostatic attraction with the protonated amine (Eq. (5)) [41]. The interaction between AuCl_4^- and the adsorption sites of the aminated PP are as follows [12,13,41].



As can be seen from Eqs. (3)–(5), the adsorption mechanism mainly involves the coordination and electrostatic attraction of the Au species with the amine functional groups of the aminated PP [42].

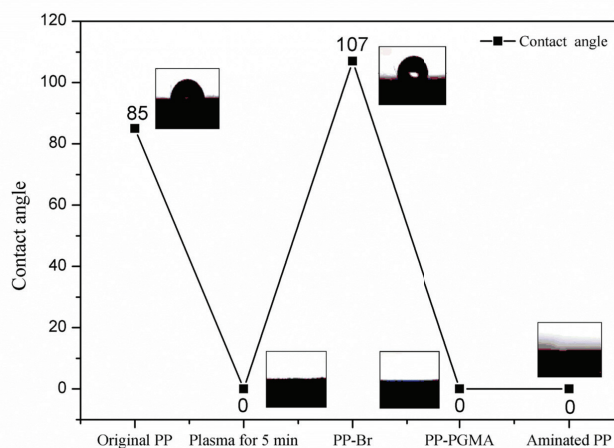


Fig. 4. Water contact angles of the membranes at each stage of the aminated PP preparation.

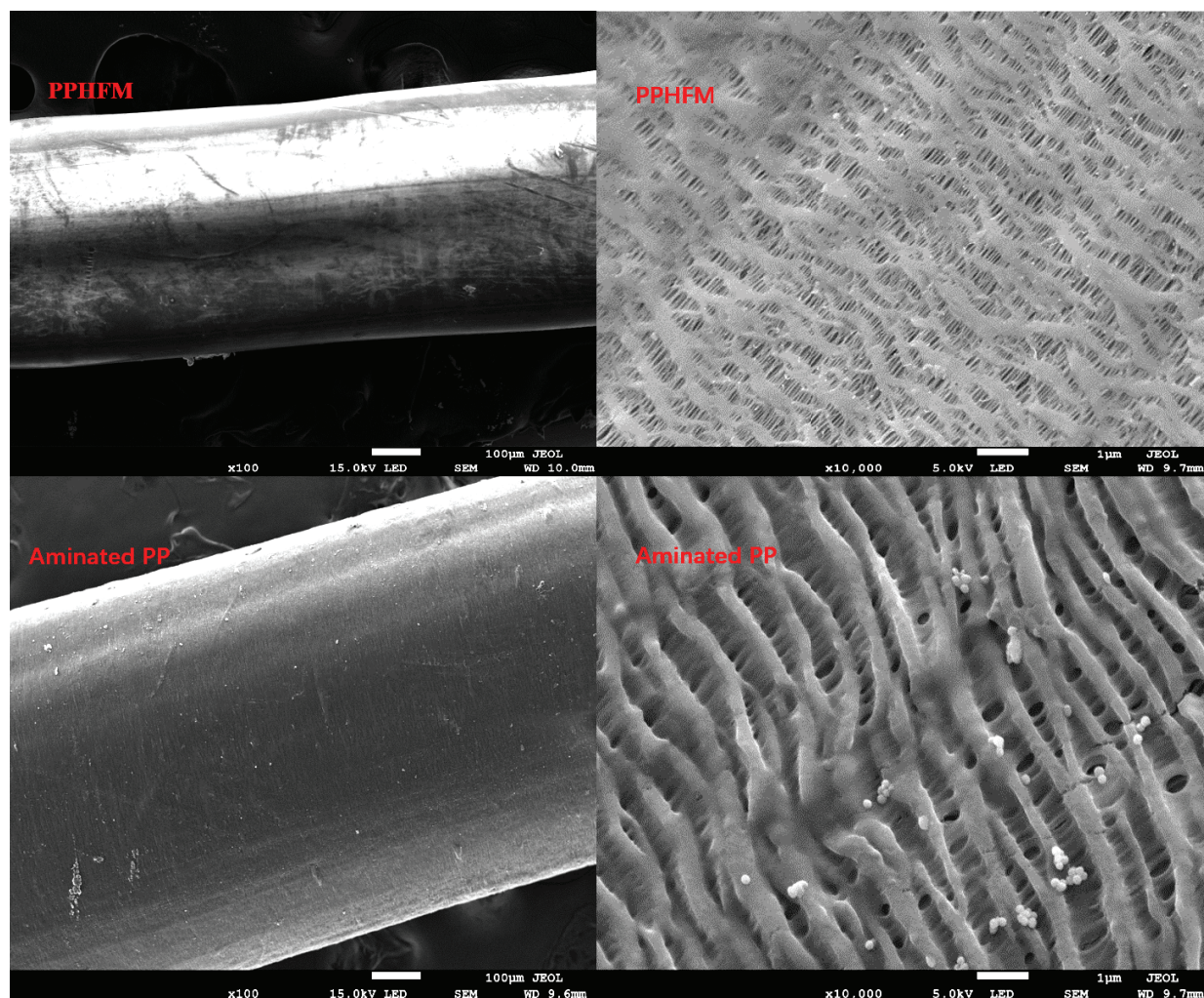


Fig. 5. FESEM images of PPHFM and the aminated PP.

3.3.2. XPS analysis

XPS was used to examine the surface element information of the aminated PP before and after Au(III) adsorption. The N1s peak was deconvoluted into sub-peaks to check the contributions of the N-containing functional groups with different oxidation state for the adsorption of Au(III). Figs. 6(a) and (b) show the XPS wide-scan spectra of the aminated PP and Au(III)-adsorbed aminated PP (PP-Au). The aminated PP clearly showed the strong N1s characteristic peak at the binding energy of 398.8 eV which proved that the amination reaction was successfully carried out on the membrane surface. In addition, the characteristic peaks of Br3d (at the binding energy of 69 eV) and Br3p (at the binding energy of 182 eV), indicated the residue BIBB initiator on the membrane surface. After the Au(III) adsorption, the Au4f peak at the binding energy of 87 eV was clearly shown in Fig. 6(b), indicating that the Au(III) was successfully adsorbed on the aminated PP surface. The N1s spectra of the aminated PP and PP-Au were further deconvoluted, as shown in Figs. 6(c) and (d). The N1s XPS spectrum of the aminated PP was deconvoluted into two sub-peaks, at the binding energy of 398.8 and 400.7 eV, respectively, representing the neutral and the protonated

amine groups, and the percentage of the protonated amine groups to the total nitrogen-containing groups was 31.3%. After the adsorption of Au(III), the percentage of the protonated amine groups was 31.1% which remained almost the same as that before the Au(III) adsorption. However, the binding energy was shifted from 400.7 to 401.6 eV, indicating that Au(III) in the form of AuCl_4^- was adsorbed onto the protonated R-NH_3^+ groups via the electrostatic attractive force. Furthermore, the binding energy of the neutral amine groups of the aminated PP was shifted from 398.8 to 399.8 eV, indicating the formation of the amine-Au(III) coordination bond with the lone-pair electrons of the nitrogen atom [11,43]. Therefore, the XPS results indicated that, at pH=2.5, both the electrostatic interaction and the coordination accounted for the adsorption of Au(III) on the aminated PP surface.

3.4. The pH effect

The effect of pH on the Au(III) adsorption performance in both single and binary metal ion species was investigated. Fig. 7(a) shows that the optimum pH appeared to be 2.0–3.0, and the maximum adsorption was obtained at pH 2.5 for Au(III). To better explain such a phenomenon, the

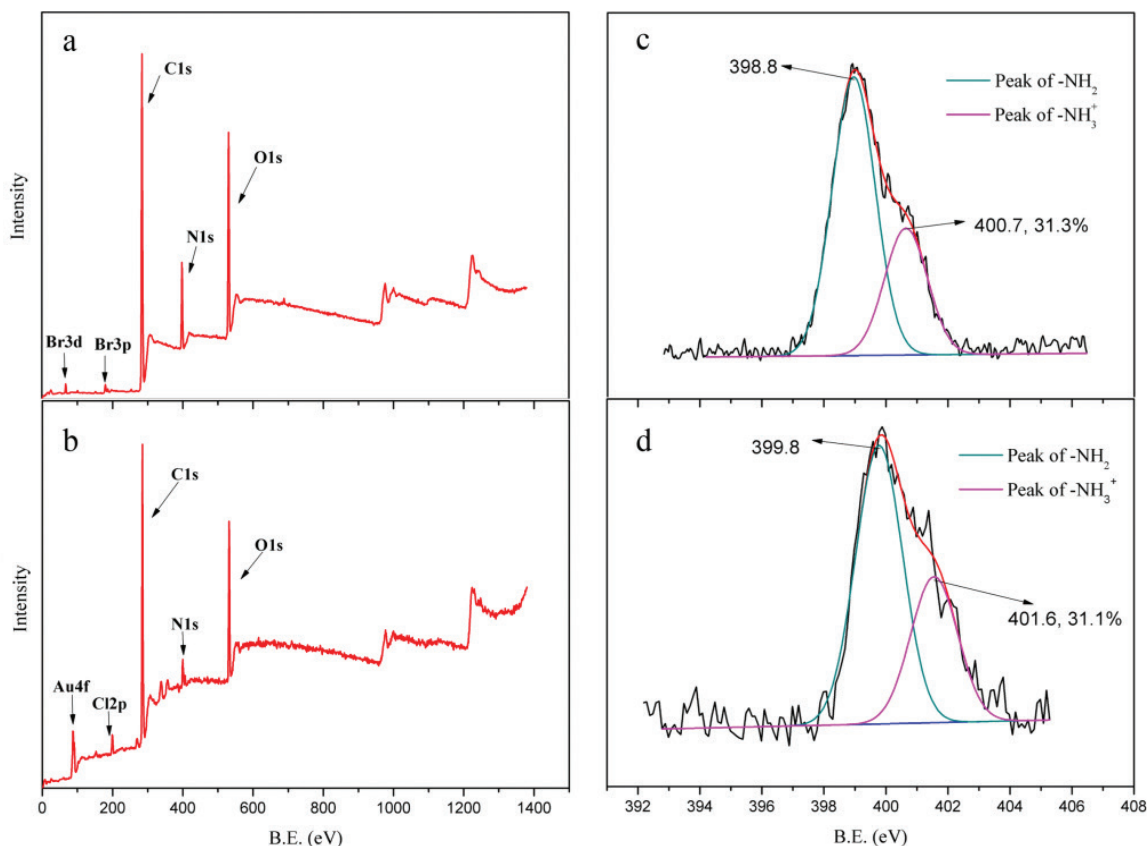


Fig. 6. (a) XPS wide-scan spectra of the aminated PP, (b) gold adsorbed aminated PP (PP-Au), (c) N1s spectra of the aminated PP at pH = 2.5, and (d) N1s spectra of the Au(III)-adsorbed aminated PP at pH = 2.5.

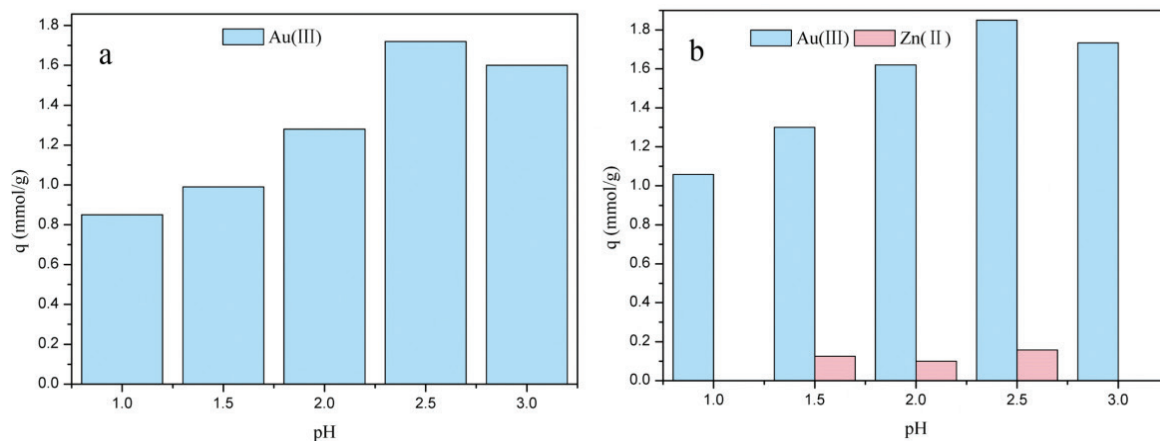


Fig. 7. (a) pH effect on the Au(III) adsorption capacity in single-species system and (b) pH effect on the Au(III) adsorption capacity in binary species system.

Table 1
The percentage of the neutral and protonated amine groups in N1s XPS core-level spectra

	pH = 1		pH = 2.5		pH = 3	
	B.E. (eV)	Percentage (%)	B.E. (eV)	Percentage (%)	B.E. (eV)	Percentage (%)
-NH ₂	399.5	66.3	399.4	68.7	399.4	81.6
-NH ₃ ⁺	401.3	33.7	401.2	31.3	401.6	18.4

B.E. – Binding energy.

deconvolution of the N1s XPS core-level spectra of the aminated PP at pH 1, 2.5, and 3 was carried out, with the results shown in Table 1. It can be seen from Table 1 that the percentage of the protonated amine groups were 33.8%, 31.3%, and 18.4% for the aminated PP at pH 1, 2.5, and 3, respectively. Although the contents of the protonated amine groups were comparable at pH 1 and 2.5, the much larger amount of Cl⁻ (hydrochloric acid was used to adjust the solution pH) at pH 1 would strongly compete with the AuCl₄⁻ ions for the adsorption sites of the protonated R-NH₃⁺ via the electrostatic interaction. As the pH gradually increased, the contents of the Cl⁻ would show a decreasing trend. As a result, the adsorption capacity of Au(III) in the form of AuCl₄⁻ ions showed an increase from pH 1 to 2.5. Further increase of the pH would drastically decrease the content of the protonated amine groups (18.4% at pH 3). Although more coordination amine sites would be generated for the complexation with Au(III), the adsorption capacity still exhibited a slight decrease due to the fact that the coordination number (the ratio of the amine groups to Au(III)) is usually more than 1 [11,43,44] in the coordination of Au(III) with the available amine sites. Therefore, the best Au(III) adsorption capacity was obtained at pH 2.5 with the aminated PP, which was similar with the pH range of 2.0–3.0 in the reported literature [45–48].

In binary species system, where both Au(III) and Zn(II) were present, the adsorption of Au(III) with the aminated PP showed the similar trend in the pH range of 1.0–3.0. In addition, the adsorption exhibited a strong selectivity toward Au(III) ions, with a little or almost no Zn(II) adsorption on the aminated PP.

3.5. Adsorption kinetics

Fig. 8(a) shows the Au(III) adsorption kinetics with the aminated PP. The adsorption was fast in the initial adsorption stage, with 1.11 mmol/g Au(III) adsorbed in the first 5 min. With the increase of the Au(III) uptake, the available adsorption sites gradually decreased, and the adsorption rate was subsequently decreased, and finally reached a plateau at 360 min with the equilibrium adsorption capacity of 1.75 mmol/g. The adsorption kinetics was further fitted with the pseudo-first-order (PFO) and pseudo-second-order (PSO) kinetics models [48–50], and the relevant calculated parameters are shown in Table 2. It was shown that the

adsorption kinetics of Au(III) was better fitted with PSO model, with the relevant coefficient (R^2) of 0.984, indicating that the chemical adsorption was predominant [51,52]. The theoretical adsorption capacity calculated with the PSO model was 1.76 mmol/g, very close to the experimental adsorption capacity (1.75 mmol/g).

The selective adsorption kinetics for Au(III) in Au(III)/Zn(II) binary species system with the aminated PP is shown in Fig. 8(b). In the initial stage, the adsorption sites were abundant and both Au(III) and Zn(II) were adsorbed on aminated PP surface. However, due to both the neutral and protonated amine sites present on the aminated PP, the Zn(II) adsorbed was much less as compared with the Au(III) adsorbed due to the electrostatic repulsive force. As the adsorption time increased, the Au(III) adsorption showed some fluctuations but kept a gradual increasing trend until the adsorption equilibrium was reached. In contrast, the Zn(II) adsorption showed a decreasing trend and almost no Zn(II) was adsorbed on aminated PP surface after 200 min. This phenomenon indicated a strong selective adsorption behavior of the aminated PP toward Au(III), that the previous adsorbed Zn(II) in the initial stage was displaced by Au(III) during the adsorption process due to the higher affinity of Au(III) toward aminated PP than that of Zn(II).

Table 2

The pseudo-first-order (PFO) and pseudo-second-order (PSO) kinetic models and model-fitting parameters for the adsorption of Au(III) with the aminated PP

Kinetics model	Model equation	Model parameters	Parameter values
PFO	$\ln(q_e - q_t) = \ln q_e - k_1 t$	k_1 (min ⁻¹)	0.007
		q_e (mmol/g)	0.819
		R^2	0.774
PSO	$t / q_t = 1 / (k_2 q_e^2) + t / q_e$	k_2 (g/mmol min)	0.029
		q_e (mmol/g)	1.761
		R^2	0.984

Note: q_t (mmol/g) and q_e (mmol/g) are the adsorption capacity at time t (min) and at the adsorption equilibrium, respectively. k_1 (min⁻¹) and k_2 (g/mmol min) are the rate constants of the PFO and PSO models, respectively. R^2 is the correlation coefficient for the relevant kinetics model equations.

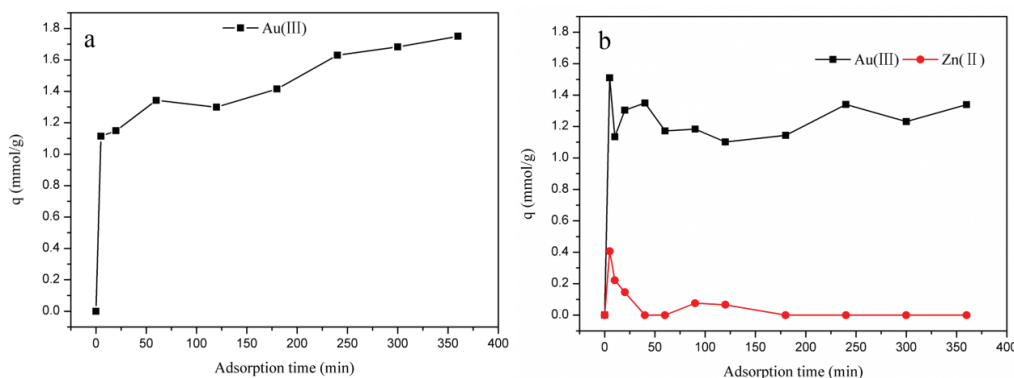


Fig. 8. (a) Adsorption kinetics of Au(III) in single-species system with the aminated PP and (b) adsorption kinetics of Au(III) and Zn(II) in the Au(III)/Zn(II) binary-species system with aminated PP.

3.6. Adsorption isotherm

The Au(III) adsorption isotherms in both single and binary species systems are shown in Figs. 9(a) and (b), respectively. Au(III) adsorption showed a sharp increase in both systems, while almost no Zn(II) was adsorbed on aminated PP in binary species system, especially at higher Zn(II) equilibrium concentrations (Fig. 9(b)). These phenomena indicated that aminated PP showed a good selectivity toward Au(III) than Zn(II). The Au(III) adsorption isotherm in single species with the aminated PP was further fitted with Langmuir and Freundlich isotherm models [12,13], which is also shown in Fig. 9(a), with the relevant equations and calculated parameters shown in Table 3. It can be seen that the adsorption isotherm was better fitted with Langmuir isotherm model with the correlation coefficient (R^2) of 0.995, indicating a single-layer adsorption with the derived maximum adsorption capacity of 2.7 mmol/g.

Table 3

The Langmuir and Freundlich adsorption isotherm models and model-fitting parameters for the adsorption of Au(III) with the aminated PP

Langmuir model			Freundlich model		
$q_e = \frac{q_m K_L C_e}{1 + K_L C_e}$			$q_e = K_F C_e^{1/n}$		
q_m (mmol/g)	K_L (L/mmol)	R^2	n	K_F ((mmol ¹⁻ⁿ L ⁿ)/g)	R^2
2.7	1.9	0.995	1.2	1.78	0.91

Note: For Langmuir model, q_e (mmol/g) and q_m (mmol/g) are the equilibrium and maximum adsorption capacity, respectively. C_e (mmol/L) is the equilibrium concentration, and K_L (L/mmol) is the Langmuir model constant. For Freundlich model, q_e and C_e have the same definitions as those of the Langmuir model. K_F ((mmol¹⁻ⁿ Lⁿ)/g) and n are the Freundlich constants, which are related to the adsorbent capacity and the adsorption intensity of the adsorbent, respectively.

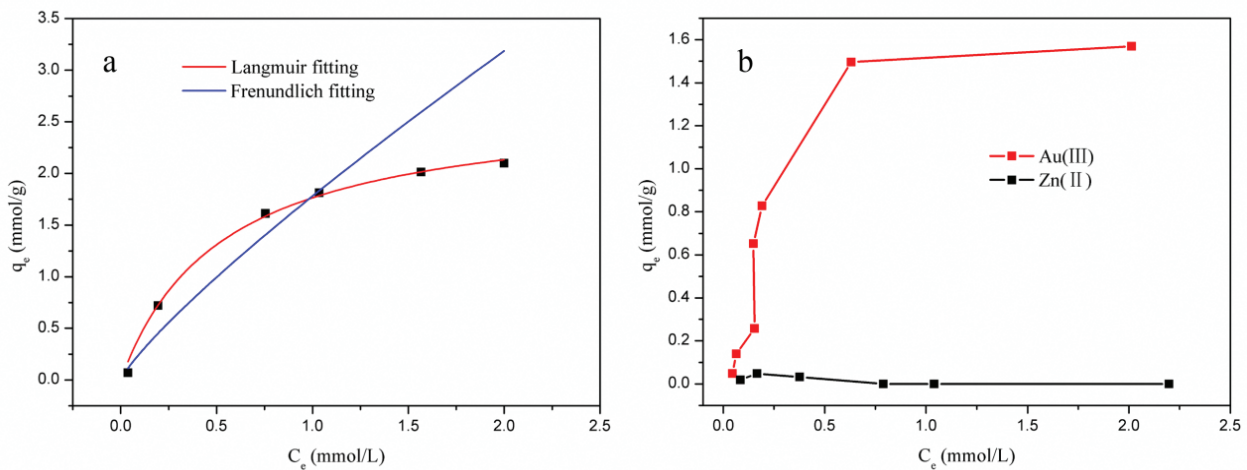


Fig. 9. (a) Langmuir and Freundlich isotherm model fitting of the Au(III) adsorption isotherm in single-species system with the aminated PP and (b) adsorption isotherms of Au(III) and Zn(II) in Au(III)/Zn(II) binary-species system with the aminated PP.

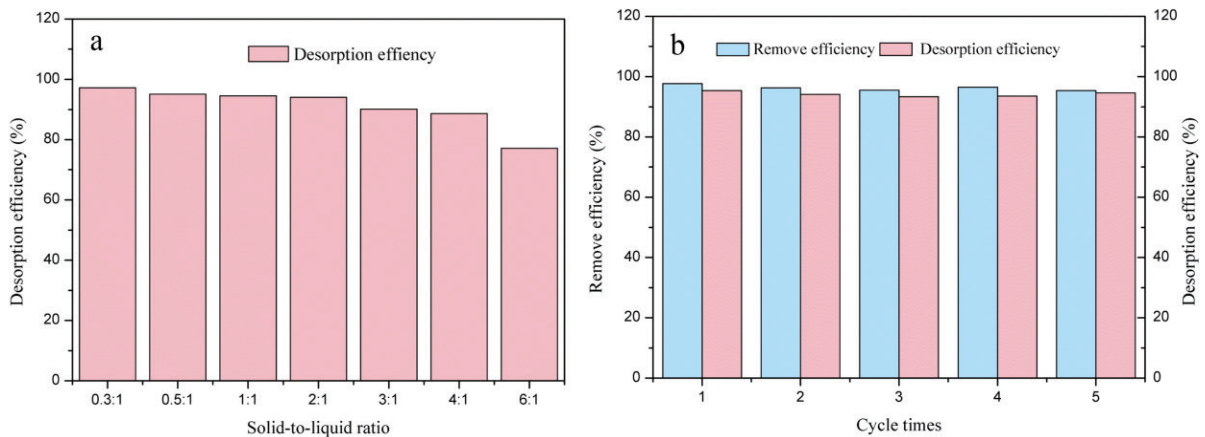


Fig. 10. (a) Desorption efficiency of Au(III) at different solid-to-liquid ratios (the ratio of the weight of the aminated PP to the volume of the thiourea solution) and (b) the effect of cycle time on the Au(III) removal efficiency and the desorption efficiency.

3.7. The desorption of Au(III)

Thiourea has a strong complexation with Au ions, and compared with cyanhydrate, it is non-toxic and environment friendly. Therefore, it is often usually used as the desorption agent for Au-adsorbed adsorbents [12]. In order to facilitate the operation and allow the aminated PP to be completely immersed in the desorption solution, the volume of the desorption solution was fixed as 20 mL, and the weight of the aminated PP was varied. Fig. 10(a) shows that the desorption efficiency gradually decreased with the increase of solid-to-liquid ratio. However, a higher desorption efficiency of more than 90% can still be achieved for the solid-to-liquid ratio of less than 6, indicating that the Au(III) adsorbed on aminated PP can be efficiently desorbed for recycling purpose. In addition, Fig. 10(b) shows that both the Au(III) removal efficiency during the adsorption process and the desorption efficiency during the desorption process were higher than 95% in the five adsorption–desorption cycles, indicating the good performance of the aminated PP for Au(III) removal and the repeated use.

4. Conclusions

In this study, the aminated polymer brush was successfully grafted onto the PPHFMs via the surface initiated radical polymerization of PGMA polymer brushes, followed by the amination with DETA. The optimum grafting and amination reaction time were found to be 4 and 12 h, respectively. The prepared aminated polypropylene membrane exhibited high selectivity and excellent adsorption capacity toward Au(III) ions at pH 2.5. The Au(III) adsorption isotherm was best fitted with the Langmuir isotherm model, and the adsorption kinetics was best described by the PSO kinetic model. A higher desorption efficiency of more than 95% was achieved for the desorption of Au(III) with the use of thiourea solutions. The adsorbent was successfully used up to five adsorption–desorption cycles without the decrease of the adsorption capacity.

Acknowledgment

This work was financially supported by the National Natural Science Foundation of China (21777105 and 51602199) and the Shenzhen Science and Technology Foundations (JCYJ20170818101137960 and JCYJ20160308105200725).

References

- [1] J. Chen, F. Saeki, B.J. Wiley, H. Cang, M.J. Cobb, Gold nanocages: bioconjugation and their potential use as optical imaging contrast agents, *Nano Lett.*, 5 (2005) 473–477.
- [2] E. Boisselier, D. Astruc, Gold nanoparticles in nanomedicine: preparations, imaging, diagnostics, therapies and toxicity, *Chem. Soc. Rev.*, 38 (2009) 1759–1782.
- [3] K.K. Turekian, K.H. Wedepohl, Distribution of the elements in some major units of the earth's crust, *Geol. Soc. Am. Bull.*, 72 (1961) 175.
- [4] L. Jarup, Hazards of heavy metal contamination, *Br. Med. Bull.*, 68 (2003) 167–182.
- [5] F. Fu, Q. Wang, Removal of heavy metal ions from wastewaters: a review, *J. Environ. Manage.*, 92 (2011) 407–418.
- [6] Y. Li, W. Zhang, Z. Long, The current status and developing trend of activated carbon regeneration in gold industry, *Gold*, 28 (2007) 32–37.
- [7] A. Dabrowski, Z. Hubicki, P. Podkościelny, E. Robens, Selective removal of the heavy metal ions from waters and industrial wastewaters by ion-exchange method, *Chemosphere*, 56 (2004) 91–106.
- [8] S.E. Baylor, T.J. Olin, R.M. Bricka, D.D. Adrian, A review of potentially low-cost sorbents for heavy metals, *Water Res.*, 33 (1999) 2469–2479.
- [9] T.A. Kurniawan, G.Y. Chan, W.H. Lo, S. Babel, Physico-chemical treatment techniques for wastewater laden with heavy metals, *Chem. Eng. J.*, 118 (2006) 83–98.
- [10] A.E. Burakov, E.V. Galunin, I.V. Burakova, A.E. Kucherova, S. Agarwal, A.G. Tkachev, V.K. Gupta, Adsorption of heavy metals on conventional and nanostructured materials for wastewater treatment purposes: a review, *Ecotoxicol. Environ. Saf.*, 148 (2018) 702–712.
- [11] L. Cao, M.C. Jennings, R.J. Puddephatt, Amine-amide equilibrium in gold(III) complexes and a gold(III)-gold(I) aurophilic bond, *Inorg. Chem.*, 46 (2007) 1361–1368.
- [12] A. Ramesh, H. Hasegawa, W. Sugimoto, T. Maki, K. Ueda, Adsorption of gold(III), platinum(IV) and palladium(II) onto glycine modified crosslinked chitosan resin, *Bioresour. Technol.*, 99 (2008) 3801–3809.
- [13] G. Lin, S. Wang, L. Zhang, T. Hu, J. Peng, S. Cheng, L. Fu, Selective recovery of Au(III) from aqueous solutions using 2-aminothiazole functionalized corn bract as low-cost bioadsorbent, *J. Cleaner Prod.*, 196 (2018) 1007–1015.
- [14] S.T. Milner, Polymer brushes, *Science*, 251 (1991) 905–914.
- [15] S. Edmondson, V.L. Osborne, W.T. Huck, Polymer brushes via surface-initiated polymerizations, *Chem. Soc. Rev.*, 33 (2004) 14–22.
- [16] K. Ohno, K. Koh, Y. Tsujii, T. Fukuda, Synthesis of gold nanoparticles coated with well-defined, high-density polymer brushes by surface-initiated living radical polymerization, *Macromolecules*, 35 (2002) 8989–8993.
- [17] R. Schmidt, T. Zhao, J.B. Green, D.J. Dyer, Photoinitiated polymerization of styrene from self-assembled monolayers on gold, *Langmuir*, 18 (2002) 1281–1287.
- [18] J. Hyun, A. Chilkoti, Surface-initiated free radical polymerization of polystyrene micropatterns on a self-assembled monolayer on gold, *Macromolecules*, 34 (2001) 5644–5652.
- [19] J. Liu, N. Feng, S. Chang, H. Kang, Preparation and characterization of poly(glycidyl methacrylate) grafted from magnesium hydroxide particles via SI-ATRP, *Appl. Surf. Sci.*, 258 (2012) 6127–6135.
- [20] X. Xu, A.M. Lenhoff, A predictive approach to correlating protein adsorption isotherms on ion-exchange media, *J. Phys. Chem. B*, 112 (2008) 1028–1040.
- [21] L. Sun, J. Dai, G.L. Baker, M.L. Bruening, High-capacity, protein-binding membranes based on polymer brushes grown in porous substrates, *Chem. Mater.*, 18 (2006) 4033–4039.
- [22] F. Xu, Q. Cai, Y. Li, E.T. Kang, K.G. Neoh, Covalent immobilization of glucose oxidase on well-defined poly(glycidyl methacrylate)-Si(111) hybrids from surface-initiated atom-transfer radical polymerization, *Biomacromolecules*, 6 (2005) 1012–1020.
- [23] F. Xu, J. Zhao, E.T. Kang, K.G. Neoh, J. Li, Functionalization of nylon membranes via surface-initiated atom-transfer radical polymerization, *Langmuir*, 23 (2007) 8585–8592.
- [24] L. Zhao, M. Li, M. Liu, Y. Zhang, C. Wu, Y. Zhang, Porphyrin-functionalized porous polysulfone membrane towards an optical sensor membrane for sorption and detection of cadmium(II), *J. Hazard. Mater.*, 301 (2016) 233–241.
- [25] L. Zhang, Y.-H. Zhao, R. Bai, Development of a multifunctional membrane for chromatic warning and enhanced adsorptive removal of heavy metal ions: application to cadmium, *J. Membr. Sci.*, 379 (2011) 69–79.
- [26] G. Bayramoglu, E. Yavuz, B.F. Senkal, M.Y. Arica, Glycidyl methacrylate grafted on p(VBC) beads by SI-ATRP technique: modified with hydrazine as a salt resistance ligand for adsorption of invertase, *Colloids Surf., A*, 345 (2009) 127–134.
- [27] J.A. Peck, C.D. Tait, B.I. Swanson, G.E. Brown, Speciation of aqueous gold(III) chlorides from ultraviolet/visible absorption and Raman/resonance Raman spectroscopies, *Geochim. Cosmochim. Acta*, 55 (1991) 671–676.

- [28] P.J. Murphy, M.S. Lagrange, Raman spectroscopy of gold chloro-hydroxy speciation in fluids at ambient temperature and pressure: a re-evaluation of the effects of pH and chloride concentration, *Geochim. Cosmochim. Acta*, 62 (1998) 3515–3526.
- [29] M. Wojnicki, E. Rudnik, M.L. Błoch, K. Paclawski, K. Fitzner, Kinetic studies of gold(III) chloride complex reduction and solid phase precipitation in acidic aqueous system using dimethylamine borane as reducing agent, *Hydrometallurgy*, 127–128 (2012) 43–53.
- [30] C. Liu, X. Liang, J. Liu, W. Yuan, Desorption of copper ions from the polyamine-functionalized adsorbents: behaviors and mechanisms, *Adsorpt. Sci. Technol.*, 34 (2016) 455–468.
- [31] J. Jia, C. Liu, L. Wang, X. Liang, X. Chai, Double functional polymer brush-grafted cotton fiber for the fast visual detection and efficient adsorption of cadmium ions, *Chem. Eng. J.*, 347 (2018) 631–639.
- [32] K. Kato, E. Uchida, E.T. Kang, Y. Uyama, Y. Ikada, Polymer surface with graft chains, *Prog. Polym. Sci.*, 38 (2003) 209–259.
- [33] M. Ejaz, S. Yamamoto, K. Ohno, Y. Tsujii, T. Fukuda, Controlled graft polymerization of methyl methacrylate on silicon substrate by the combined use of the Langmuir-Blodgett and atom transfer radical polymerization techniques, *Macromolecules*, 31 (1998) 5934–5936.
- [34] G. Bayramoglu, B. Altintas, M.Y. Arica, Adsorption kinetics and thermodynamic parameters of cationic dyes from aqueous solutions by using a new strong cation-exchange resin, *Chem. Eng. J.*, 152 (2009) 339–346.
- [35] R.K. Sharma, Lalita, A.P. Singh, G.S. Chauhan, Grafting of GMA and some comonomers onto chitosan for controlled release of diclofenac sodium, *Int. J. Biol. Macromol.*, 64 (2014) 368–376.
- [36] C. Liu, R. Bai, L. Hong, Diethylenetriamine-grafted poly(glycidyl methacrylate) adsorbent for effective copper ion adsorption, *J. Colloid Interface Sci.*, 303 (2006) 99–108.
- [37] P. Liu, Y. Liu, Z. Su, Modification of poly (hydroethyl acrylate)-grafted cross-linked poly (vinyl chloride) particles via surface-initiated atom-transfer radical polymerization, *Ind. Eng. Chem. Res.*, 45 (2006) 2255–2260.
- [38] S. Deng, G. Yu, S. Xie, Q. Yu, J. Huang, Enhanced adsorption of arsenate on the aminated fibers: sorption behavior and uptake mechanism, *Langmuir*, 24 (2008) 10961–10967.
- [39] J.F. Hester, P. Banerjee, Y.Y. Won, A. Akthakul, ATRP of amphiphilic graft copolymers based on PVDF and their use as membrane additives, *Macromolecules*, 35 (2002) 7652–7661.
- [40] L.Q. Huang, S.J. Yuan, L. Lv, G.Q. Tan, B. Liang, S.O. Pehkonen, Poly (methacrylic acid)-grafted chitosan microspheres via surface-initiated ATRP for enhanced removal of Cd(II) ions from aqueous solution, *J. Colloid Interface Sci.*, 405 (2013) 171–182.
- [41] S. Boufia, M.R. Vilar, A.M. Ferrariac, A.M. Botelho, In situ photochemical generation of silver and gold nanoparticles on chitosan, *Colloids Surf., A*, 439 (2013) 151–158.
- [42] P. Chassarya, T. Vincenta, J.S. Marcanob, L.E. Macaskiec, E. Guibal, Palladium and platinum recovery from bicomponent mixtures using chitosan derivatives, *Hydrometallurgy*, 76 (2005) 131–147.
- [43] R.L. Monica, P.V. Bernhardt, A.L. Geoffrey, M. Marcel, Gold(III) template synthesis of a pendant-arm macrocycle, *J. Chem. Soc., Dalton Trans.*, 1 (1997) 323–327.
- [44] T. Kanjiro, S. Akihiro, E. Kunio, Au(III)-PAMAM interaction and formation of Au-PAMAM nanocomposites in ethyl acetate, *J. Colloid Interface Sci.*, 241 (2001) 346–356.
- [45] M.L. Arrascue, H.M. Garcia, O. Horna, E. Guibal, Gold sorption on chitosan derivatives, *Hydrometallurgy*, 71 (2003) 191–200.
- [46] E. Guibal, A. Larkin, T. Vincent, J.M. Tobin, Chitosan sorbents for platinum sorption from dilute solutions, *Ind. Eng. Chem. Res.*, 38 (1999) 4011–4022.
- [47] A. Uheida, M. Iglesias, C. Fontas, M. Hidalgo, V. Salvado, Sorption of palladium(II), rhodium(III), and platinum(IV) on Fe₃O₄ nanoparticles, *J. Colloid Interface Sci.*, 301 (2006) 402–408.
- [48] S. Luo, X. Xu, G. Zhou, C. Liu, Y. Tang, Y. Liu, Amino siloxane oligomer-linked graphene oxide as an efficient adsorbent for removal of Pb(II) from wastewater, *J. Hazard. Mater.*, 274 (2014) 145–155.
- [49] Y.S. Ho, G. McKay, Pseudo-second order model for sorption processes, *Process Biochem.*, 34 (1999) 451–465.
- [50] C. Liu, J. Jia, J. Liu, X. Liang, Hg selective adsorption on polypropylene-based hollow fiber grafted with polyacrylamide, *Adsorpt. Sci. Technol.*, 36 (2018) 287–299. doi: 10.1177/0263617416689480.
- [51] L. Zheng, Z. Dang, X. Yi, H. Zhang, Equilibrium and kinetic studies of adsorption of Cd(II) from aqueous solution using modified corn stalk, *J. Hazard. Mater.*, 176 (2010) 650–656.
- [52] V. Soni, R.N. Mehrotra, Kinetics and mechanism of oxidation of hydroxylamine by tetrachloroaurate(III) ion, *Transition Met. Chem.*, 28 (2003) 893–898.